Title

Increase in relative deposition of fine particles in the rat lung periphery in the absence of gravity

Journal

Journal of Applied Physiology, 117(8)

ISSN

8750-7587

Authors

Darquenne, Chantal
Borja, Maria G
Oakes, Jessica M
et al.

Publication Date

2014-10-15

DOI

10.1152/japplphysiol.00298.2014

Peer reviewed

J Appl Physiol 117: 880–886, 2014.
First published August 28, 2014; doi:10.1152/japplphysiol.00298.2014.

Increase in relative deposition of fine particles in the rat lung periphery in the absence of gravity

Chantal Darquenne,[1] Maria G. Borja,[2] Jessica M. Oakes,[2] Ellen C. Breen,[1] I. Mark Olfert,[1] Miriam Scadeng,[3] and G. Kim Prisk[1,3]

[1]*Department of Medicine, University of California, San Diego, La Jolla, California;* [2]*Department of Mechanical and Aerospace Engineering, University of California, San Diego, La Jolla, California; and* [3]*Department of Radiology, University of California, San Diego, La Jolla, California*

Submitted 3 April 2014; accepted in final form 21 August 2014

Darquenne C, Borja MG, Oakes JM, Breen EC, Olfert IM, Scadeng M, Prisk GK. Increase in relative deposition of fine particles in the rat lung periphery in the absence of gravity. *J Appl Physiol* 117: 880–886, 2014. First published August 28, 2014; doi:10.1152/japplphysiol.00298.2014.—While it is well recognized that pulmonary deposition of inhaled particles is lowered in microgravity (μG) compared with gravity on the ground (1G), the absence of sedimentation causes fine particles to penetrate deeper in the lung in μG. Using quantitative magnetic resonance imaging (MRI), we determined the effect of gravity on peripheral deposition ($DEP_{peripheral}$) of fine particles. Aerosolized 0.95-μm-diameter ferric oxide particles were delivered to spontaneously breathing rats placed in plethysmographic chambers both in μG aboard the NASA Microgravity Research Aircraft and at 1G. Following exposure, lungs were perfusion fixed, fluid filled, and imaged in a 3T MR scanner. The MR signal decay rate, R_2*, was measured in each voxel of the left lung from which particle deposition (DEP) was determined based on a calibration curve. Regional deposition was assessed by comparing DEP between the outer ($DEP_{peripheral}$) and inner ($DEP_{central}$) areas on each slice, and expressed as the central-to-peripheral ratio. Total lung deposition tended to be lower in μG compared with 1G (1.01 ± 0.52 vs. 1.43 ± 0.52 μg/ml, $P = 0.1$). In μG, $DEP_{peripheral}$ was larger than $DEP_{central}$ ($P < 0.03$), while, in 1G, $DEP_{peripheral}$ was not significantly different from $DEP_{central}$. Finally, central-to-peripheral ratio was significantly less in μG than in 1G ($P \leq 0.05$). These data show a larger fraction of fine particles depositing peripherally in μG than in 1G, likely beyond the large- and medium-sized airways. Although not measured, the difference in the spatial distribution of deposited particles between μG and 1G could also affect particle retention rates, with an increase in retention for particles deposited more peripherally.

lunar dust; MRI; aerosol; microgravity

ONE OF THE MANY HAZARDS FACING future explorers to the surface of the Moon is lunar dust. Lunar dust is persistently adhesive and abrasive due to its combined physical and electrical properties (3) and is also thought to be highly reactive in nature as the exposed surfaces are analogous to terrestrial fresh fractured quartz (4). Because a significant fraction of lunar dust is in the inhalable and respirable range (17), it has the potential to pose a significant threat to the pulmonary health of human explorers. Experience in the Apollo explorations showed that lunar dust was pervasive and readily transported into the habitat. This resulted in astronauts being exposed to the dust for several days (15, 23).

Address for reprint requests and other correspondence: C. Darquenne, Univ. of California, San Diego, 9500 Gilman Dr., #0623A, La Jolla, CA 92093-0623 (e-mail: cdarquenne@ucsd.edu).

The deposition of particles between 0.5 and 3 μm in the lung is strongly influenced by gravitational sedimentation. Studies by our group have shown that deposition in both microgravity (μG) and lunar gravity (1/6G) is substantially lower than in normal gravity (1G) (5, 8, 9, 11–13). While total deposition is lowered by reduced gravity, the reduction in sedimentation also means that particles that would normally be deposited in proximal airways in 1G remain in suspension and are subsequently transported to the peripheral lung, where they eventually deposit and where clearance mechanisms are slower, likely resulting in longer residence times for deposited particles.

Our laboratory has recently developed a MRI-based method capable of quantifying the spatial distribution of deposited particles in small animals (28). The technique uses the change in magnetic resonance (MR) signal decay rate (R_2*) between lungs exposed to iron oxide particles and control lungs (no aerosol exposure) to quantify the number of particles deposited in different lung regions. The technique has been successfully used in both healthy (28) and emphysematous animals (26).

The goal of this study was to measure the regional distribution of deposited particles following exposure of spontaneously breathing rats to aerosolized 0.95-μm-diameter iron oxide particles, both on the ground (1G) and in μG during parabolic flights. All but one (14) of our laboratory's previous studies of aerosol deposition in altered gravity (8–13, 30) was performed using photometer techniques that did not provide information on the spatial location of deposited particles. Such information is essential for determining particle retention rates in the lung and is the focus of this study. Because the gravity level directly affects deposition by sedimentation, we hypothesized that, in a reduced gravity environment, total deposition may be somewhat decreased, but those particles that do deposit will do so more peripherally.

METHODS

Aerosol exposure and protocol. The study protocol was approved by the Institutional Animal Care and Use Committees at the University of California, San Diego (UCSD), at NASA Johnson Space Center in Houston, TX, and at NASA Ames Research Center in San Jose, CA. The studies were performed in 18 male healthy adult Wistar rats (260 ± 9 g). The equipment allowed for four rats to be simultaneously restrained in individual plethysmographic chambers (Buxco Research Systems, Wilmington, NC) (Fig. 1). The chambers were continuously ventilated, with either clean or particle-laden air at a rate of ~2.4 l/min, while the animals' breathing patterns (i.e., tidal volume and breathing frequency) were continuously recorded (BioSystemXA, Buxco Research Systems, Wilmington, NC). The animals were positioned in the chamber such that their nose was directly facing the incoming flow of air. The aerosol delivery system allowed for rapid

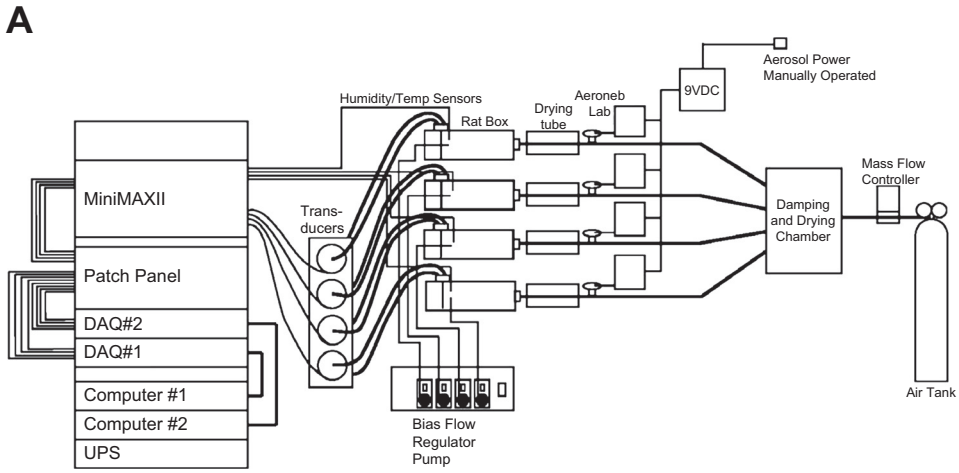

Fig. 1. Equipment. *A*: schematic representation of experimental equipment. Animals are housed in plethysmographic chambers (rat box) with their nose facing the incoming flow. A manually operated switch allowed for powering on the vibrating mesh nebulizers (Aeroneb Lab). Aerosol flows through a drying tube to remove the water droplets so that an aerosol made of dry particles flows in the animal chambers. All relevant data from the pressure transducers, temperature and humidity probes, and accelerometer are collected twice (to provide a redundant data backup) using two analog-to-digital systems DAQ#1 and DAQ#2 (National Instruments, Austin, TX) in rack-mounted computers (Dell, Round Rock, TX). UPS, uninterruptible power supply. MiniMaxII: Preamplifier unit. *B*: picture of the animal rack that could house four animals simultaneously.

activation and deactivation of the particle supply so that animals were only exposed to particles during the μG phase of the parabolic flight and breathed particle-free air at all other times. Deactivation of the aerosol supply was performed about 5 s before the end of each μG phase to allow for the dead space between the aerosol nebulizer and the nose of the animals to be flushed with particle-free air before the change in gravity level. Each parabola provided ~25 s of reduced gravity, giving a cumulative exposure period of ~14 min in a typical flight of 40 parabolas. At the end of each flight, animals were immediately taken to laboratory facilities at the Johnson Space Center, where they were given a lethal dose of Euthasol before fixation of their lungs by vascular perfusion. Like in our laboratory's previous studies (26, 28), fixation by vascular perfusion was preferred over fixation by tracheal instillation to minimize any potential dislocation of deposited particles during the fixation process. The time between end of aerosol exposure and lung fixation was 86 ± 11 min. Fixed lungs were then stored in jars filled with fixative and shipped to UCSD, where they were imaged at the UCSD center for functional MRI.

Control studies at 1G were performed after the μG studies so that the timing of the exposures and lung fixations could be matched to that of the parabolic flight studies (a delayed synchronous control approach). Control studies were performed with the same equipment and in the same configuration as during the μG studies. It should also be noted that, because of the delay between the end of aerosol exposure and the lung fixation, it is likely that most of the particles that deposited in the large airways had cleared before fixation (1), affecting the measure of spatial distribution of deposited particles within the lung. This is, however, expected to have a minimal effect on our results, because the volume of proximal airways only represents a small fraction of total lung volume (<3%).

While it was originally planned to study 12 animals in each group, severe weather prevented us from completing the parabolic flights as planned, and only six animals were studied in each group.

Aerosol generation. The aerosol used in this experiment was made of monodisperse magnetic polystyrene particles with a diameter of 0.95 μm (coefficient of variation <5%) and a density of 1.35 g/cm^3 (Kisher Biotech, Steinfurt, Germany). The particles, made by coating polystyrene core particles with a layer of iron oxide and polystyrene, were supplied in aqueous solution (25 mg/ml water). The solution was diluted in a 1:20 ratio with water and nebulized into an aerosol with four vibrating mesh nebulizers (Aeroneb, Galway, Ireland), one per plethysmographic chamber. Data from a previous study (14) in μG showed no significant difference in the generation and size of droplets obtained by a vibrating mesh generator in μG and in 1G. Measurements using a Sierra Series 210 eight-stage cascade impactor (Sierra Instruments, Carmel Valley, CA) showed a size of 4.9 μm (mass median aerodynamic diameter) with a geometric standard deviation of 2.5 in 1G and a mass median aerodynamic diameter of 5.6 μm with a geometric standard deviation of 2.4 in μG.

To remove water droplets, the aerosol flowed through a heated tube and a diffusion dryer before reaching the animal chamber so that the resulting aerosol was made of dry magnetic particles of uniform size. The dried aerosol was checked on the ground before the study with a particle sizer (APS3321, TSI). Size analysis showed that the fraction of doublets and triplets in the aerosol was negligible with a mean geometric diameter of 0.93 μm.

Lung preparation for imaging. Following aerosol exposure, rats were given 500 units of heparin intraperitonally to inhibit intravascular blood coagulation, followed by a lethal dose of Euthasol (pentobarbital sodium 390 mg/ml + phenytoin sodium 50 mg/ml). The lungs were then fixed by vascular perfusion through the pulmonary artery (28). A mixture of heparin and saline (1 ml heparin/100 ml saline) was first infused for 5 min to clear blood from the lungs, followed by fixative (3% glutaraldehyde solution in 0.01 M phosphate buffer) for 15 min at a flow rate of 10–15 ml/min and an airway pressure of 20 cmH_2O. Lungs were then excised and stored in fixative.

Imaging. The imaging protocol was the same as described previously in detail (26, 28). Briefly, the lungs were placed in MR-compatible container that could hold three sets of lungs. Lungs were immersed in fixative and held in place with gauze. Each container was degassed under a light vacuum for ~2 wk until all air bubbles were removed from the lungs. Before imaging, the MR compatible container was placed in the center of a large cylindrical plastic vessel filled with water. The large vessel of water reduced the field inhomogeneities that would otherwise be present at the interface of the MR container and air (28). Lungs were imaged with a 3T General Electric (GE) Signa HDX MR scanner using a GE 18-cm-diameter transmit and receive knee coil. A gradient echo sequence was used with a flip angle of 20°, a repetition time of 2 s, a field of view of 13 cm, and echo times of 8.2, 40, 100, and 200 ms. Approximately 32 transaxial images were obtained with an in-plane resolution of 500 μm and thickness of 1 mm. Figure 2 shows representative axial MR images of the MR-compatible container housing three sets of lungs each.

Data analysis. Data analysis was performed as previously described (26, 28). Briefly, the signal R_2* was measured in each voxel of the left lung. The concentration of deposited particles (DEP) was then calculated using a calibration curve between R_2* and DEP that was obtained previously by imaging phantoms with known particle concentrations using the same MR sequence (28). Regions of interest delimiting the central and peripheral regions were hand-drawn and defined as follows (28): for the axial slices located in the midportion of the lung, both a central and peripheral region were defined on each slice, as shown in Fig. 2, while the axial slices located at the apex and the base of the lung only included peripheral tissue. The central region was then added together to form a three-dimensional central region. Similarly, all peripheral regions were added together to form a three-dimensional peripheral region. As a result, the central region made up ~25% of the lung, with the remaining 75% consisted of the peripheral region. Regional deposition (DEP) was then assessed by comparing DEP values between the peripheral ($DEP_{peripheral}$) and central ($DEP_{central}$) areas on each slice, and was expressed as the central-to-peripheral (C/P) ratio. Analysis of the left lung only was considered representative of deposition in the whole lung. This is based on a recent study by our group (26) that used the same particles as in the present study, where no difference in the DEP between lobes of healthy rat lungs was found.

Statistical analysis. All statistical analyses were performed with Systat version 11 (Systat, Evanston, IL). Data were grouped in different categorical variables: experimental condition (control, exposed 1G, exposed μG), lung region (whole, central, and peripheral), and animal number. A two-way analysis of variance was performed to test for differences in total and regional deposition (Figs. 3 and 4). Post hoc testing using the Bonferroni adjustment was performed for tests showing significant *F*-ratios. A standard *t*-test was used to test for differences in breathing parameters (tidal volume and breathing frequency) and C/P ratio (Fig. 5) between G levels. Significant differences were accepted at the $P \leq 0.05$ level.

RESULTS

Respiratory parameters. There were no significant differences in the breathing parameters of the rats exposed to particles in μG or in 1G. Tidal volume was 1.22 ± 0.43 ml (mean ± SD) in μG and 1.45 ± 0.33 ml in 1G ($P = 0.41$). Breathing frequency was 107 ± 12 min^{-1} in μG and 111 ± 16 min^{-1} in 1G ($P = 0.64$). Minute volume was 131 ± 33 ml/min in μG and 159 ± 42 ml/min in 1G ($P = 0.29$). Based on its tidal volume (~2 ml), one animal in the μG group was considered an outlier (Grubbs test) and was removed from the data analysis.

Deposition. Data are presented for six controls (no aerosol exposure), and five rats in each of the exposed groups (1G and μG). One rat was removed from the μG group because it was considered an outlier based on its tidal volume (see above), and one rat was removed from the 1G group because blood could

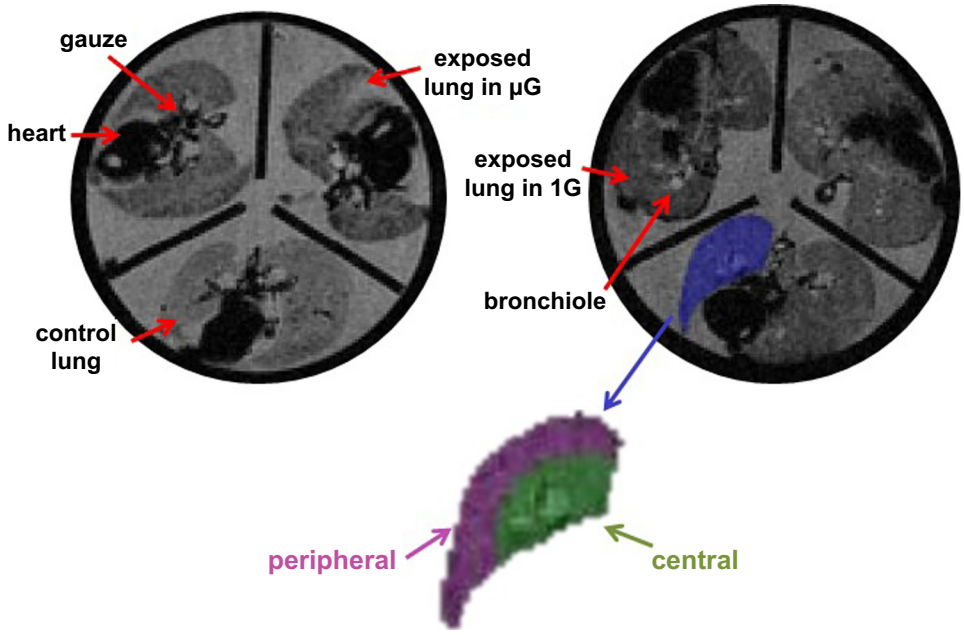

Fig. 2. Representative signal intensity images of rat lungs from the microgravity (μG; *left*) and gravity on the ground (1G) studies (*right*). Each image showed three sets of rat lungs house in the magnetic resonance (MR)-compatible container used during the MR imaging sessions. Both control (no particle exposure) and aerosol-exposed lungs are identified on the figure. The lung outlined in blue is an example of a region of interest (ROI) drawn for the left lung. The peripheral (purple) and central (green) ROI are also shown.

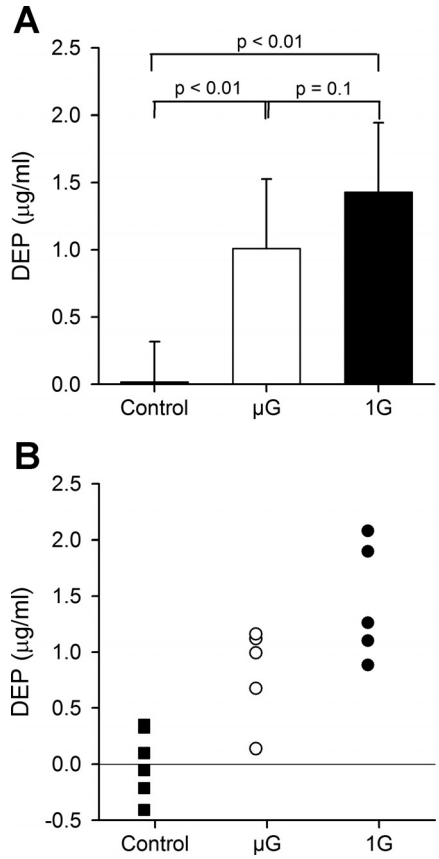

Fig. 3. Deposition in the entire lung in μG and 1G. Data from the control animals (no exposure) are also shown. Significant deposition was found in both exposed groups with a trend for deposition to be higher in 1G than in μG. *A*: data averaged over all animals in each group (mean ± SD). *B*: individual data in each group. DEP, concentration of deposited particles.

not be completely cleared from its lung during the fixation process.

The DEP for animals exposed in μG and 1G is shown in Fig. 3, along with the data from the control group (no aerosol exposure). Concentration is expressed in micrograms per milliliter lung volume. For the average particle size used in this study (i.e., a diameter of 0.95 μm and a density of 1.35 g/cm^3), a concentration of 1 μg/ml is equivalent to ~200,000 particles depositing on the air space walls contained in a 1-ml volume of the lung. Significant deposition was found in both exposed groups with a trend for deposition to be higher in 1G than in μG (1.43 ± 0.52 vs. 1.01 ± 0.52 μg/ml, $P = 0.1$).

Regional deposition averaged over all animals (mean ± SD) in both μG and 1G are shown in Fig. 4*A*. Individual data are shown in Fig. 4, *B* and *C*, for lungs exposed in μG and 1G, respectively. The relative regional volume of the peripheral region was 73 ± 4 and 72 ± 3% for the lungs exposed in μG and 1G, respectively. While there was no regional difference in deposition for animals exposed in 1G, $DEP_{central}$ was significantly less than $DEP_{peripheral}$ in μG ($P < 0.03$, Fig. 4). There was also a trend for $DEP_{central}$ to be less in μG than in 1G ($P = 0.07$), while there was no difference in $DEP_{peripheral}$ between the two gravity levels. Finally, the effect of gravity on the C/P ratio is shown in Fig. 5, where both averaged (mean ± SD) and individual data are shown. C/P significantly decreased from 0.92 ± 0.23 in 1G to 0.65 ± 0.23 in μG ($P \leq 0.05$).

DISCUSSION

In this study, we used inhalation of iron oxide fine particles and quantitative MRI to study the effect of gravity on aerosol deposition patterns in healthy lungs of rats exposed to particles either in μG or in 1G. The spatial distribution of deposited particles was assessed postmortem in excised fixed lungs. This is one of the first studies that directly measure the effect of gravity on the site of regional deposition in the lung. Indeed,

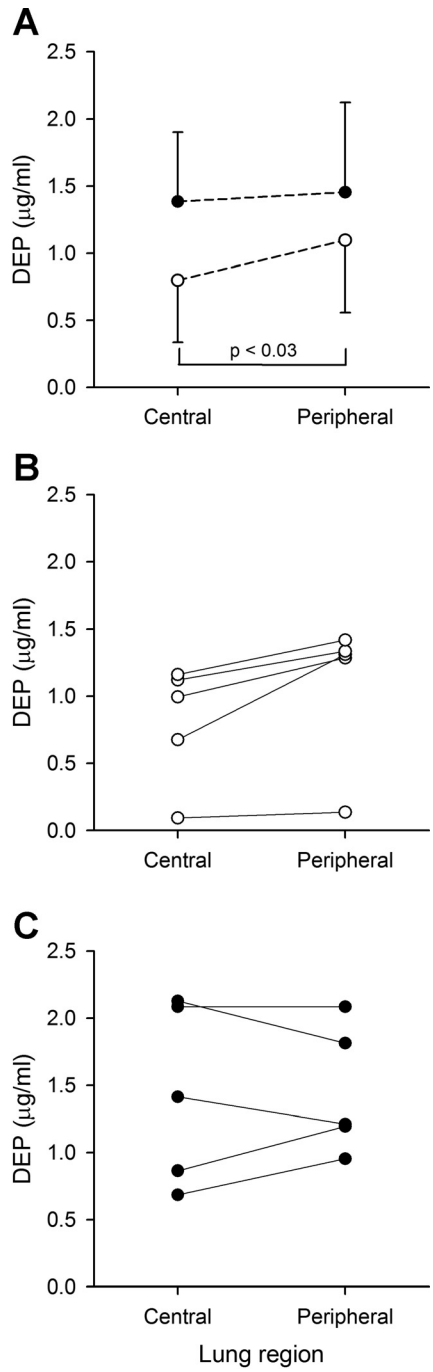

Fig. 4. DEP in the central and peripheral region of animals exposed in μG (○) and 1G (●). *A*: data averaged over all animals in each group (mean ± SD). For clarity purposes, only one-sided error bars are shown on the figure. *B*: individual data for animals exposed in μG. *C*: individual data for animals exposed in 1G.

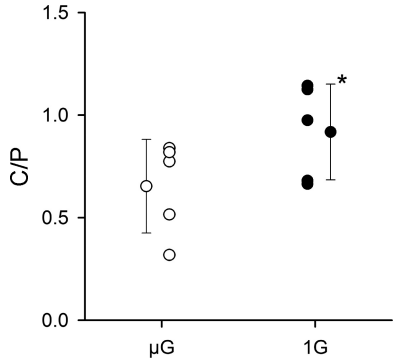

Fig. 5. Effect of gravity on the central-to-peripheral (C/P) ratio. Both individual and averaged data (mean ± SD) are shown for each group. *Significantly different ($P \leq 0.05$) from μG data.

most of the previous studies in altered gravity used photometer techniques that do not provide spatial information on the location of deposited particles (7–13, 30). Rather, the photometer technique provides either overall deposition during continuous aerosol inhalation or infers regional deposition by probing different volumetric depths of the lung with aerosol boluses. Even though no spatial information was available, measurements from aerosol bolus inhalations provided indirect evidence that deposition of fine particles in the lung periphery was likely enhanced in reduced gravity compared with 1G (9, 11). The MRI technique used in this study allowed for a direct assessment of the effect of gravity on the three-dimensional distribution of deposited particles in the rat lung at a resolution of 0.5 mm^3.

Overall deposition. Our data showed a trend for overall deposition to be less in μG than in 1G (Fig. 3). Although not statistically significant, the minute volume of aerosol inhaled in μG was less than that inhaled in 1G by ~18%. Figure 3 shows an average decrease in deposition between 1G and μG of ~30%. The larger decrease in deposition than in minute volume suggests that the rate of deposition in μG was likely less than in 1G, in agreement with previous measurements made by our group in humans (8). In that previous study, we measured the deposition of 0.5- to 3-μm-diameter particles in μG, 1G, and 1.6 G and showed that, for all particle sizes, deposition increased with increasing gravity level. While deposition of 2- and 3-μm particles was significantly different between all gravity levels, deposition of 0.5- and 1-μm particles was only significantly increased between μG and 1.6 G with a trend for increased deposition between μG and 1G. Even though there are major differences between rats and humans, in terms of both airway tree structure (27, 39) and ventilation distribution between dependent and nondependent regions of the lungs (16, 32), the human data obtained with fine particles (i.e., 0.5 and 1 μm) agree well with the observations made in the rat lungs in the present study. Indeed, for the 1-μm particles, deposition in μG was 77% of that measured in 1G in humans (8) and was 71% in rats (Fig. 3). Furthermore, based on previous experimental studies in spontaneously breathing rats (31) and on predictions from the International Commission on Radiological Protection model of the human respiratory tract for resting nose breathing conditions (20), the relative distribution of intrathoracic deposition between the tracheobronchial and alveolar region is remarkably similar for the human and rat lung with ~75% of deposited particles located in the alveolar region. Although overall absolute deposition is larger in human than in rat lungs, such similarity in the relative distribution of deposited particles makes the rat lung an attractive model for toxicological studies.

Regional deposition. The data show that the relative distribution of deposited particles between the central and peripheral region of the rat lung is affected by gravity. In μG, $DEP_{central}$ was significantly less than $DEP_{peripheral}$, while in 1G, there was no difference in deposition between the two regions (Fig. 4). This resulted in a C/P ratio that was less in μG than in 1G (Fig. 5). These data agree with the indirect assessment from bolus tests that suggested that the removal of gravity would result in relative deposition of fine particles being greater in the lung periphery than in the central airways (9, 11). It should be emphasized that this observation is valid only for fine particles. Indeed, a previous study in humans by our group using planar gamma scintigraphy has shown that the absence of gravity reduced the relative deposition of coarse particles (~5 μm) in the lung periphery, causing C/P to be larger in μG than in 1G (14). That was the direct result of a decrease in $DEP_{peripheral}$ in the absence of gravitational sedimentation rather than an increase in $DEP_{central}$, where deposition was dominated by inertial impaction, a mechanism unaffected by gravity. In the case of fine particles for which inertial impaction is negligible, our data suggest that the change in the C/P ratio between gravity levels results from a decrease in $DEP_{central}$ in μG (Fig. 4).

Interestingly, even though sedimentation is absent in μG, $DEP_{peripheral}$ of fine particles was almost the same in both gravity levels (Fig. 4). This suggests that other deposition mechanisms than gravitational sedimentation must play a significant role in the lung periphery when gravity is removed. Potential mechanisms include convective mixing and particle trapping in the alveolar spaces.

Convective mixing refers to the transport mechanisms, except Brownian diffusion, that irreversibly transfer inspired air into resident air (19). Factors contributing to convective mixing include nonhomogeneous ventilation of the lung (13, 33), nonreversibility of velocity profiles within the air spaces, airway and alveolar geometries asymmetries between inspiratory and expiratory flows (34), cardiogenic mixing (7, 30, 35), and the phenomenon of "stretch and fold" (2, 10). The concept of stretch and fold was introduced by Butler and Tsuda (2) and addresses the mechanism of complex mixing that is thought to occur in the acinus as a result of the rhythmical expansion and contraction of complex alveolar structures. Using flow visualization techniques in a rat lung, they demonstrated that the reciprocal motion of the air in the airways wraps the streamlines around each other during tidal breathing. Initially widely separated streamlines are brought into close apposition with each other, while previously close streamlines tend to diverge from one another. As such, geometrically long diffusion distances are greatly reduced, and the effect is that of an increase in the apparent diffusion coefficient, potentially contributing to acinar mixing and enhanced deposition. Our laboratory previously showed in a study in μG that the phenomenon of stretch and fold was an operative mechanism in aerosol mixing in humans (10). Although not definitive of the concept, those data strongly suggested that the phenomenon of stretch and fold already occurred during one single flow reversal in the human lung, a conclusion consistent with *1*) the complex mixing

pattern seen in polymer filled rat lungs after a single breathing cycle (38); *2*) the high degree of dispersion and deposition previously observed with single bolus inhalations in μG (7, 12, 13); and *3*) the high $DEP_{peripheral}$ reported in this study.

Previous modeling studies (6, 24, 29) have shown that a significant number of inhaled fine particles (0.5–1 μm) remain in suspension in the acinar region of the lung at the end of a breathing cycle. These trapped particles eventually deposit during subsequent breathing cycles by either sedimentation (in 1G) or following complex alveolar mixing resulting from the rhythmic motion of the alveolar walls. A third mechanism that could be significant is that of geometrical interception, which has been shown to significantly contribute to alveolar deposition under μG conditions (18). While deposition due to alveolar mixing and/or geometrical interception in the lung periphery might be masked by the dominating effect of sedimentation in 1G, the observation of almost similar levels of $DEP_{peripheral}$ in μG and 1G (Fig. 4) strongly suggests that these are important gravity-independent mechanisms of fine-particle aerosol deposition.

Relevance to toxicological studies of extraterrestrial dust. To date, much of the assessment of pharmacological and toxicological effects of inhaled particles comes from studies in small rodents (1). The study of the toxicological effects of Lunar or Mars dust is no exception. Lam et al. (21, 22) have used tracheal instillation in mice to study the pulmonary toxicity of simulated Lunar and Martian dusts. They observed focal regions of particulate-laden macrophages, mild-to-moderate focal alveolitis, and perivascular and peribronchiolar inflammation as early as 7 days following exposure, and chronic pulmonary inflammation, alveolar septal thickening, and fibrosis 90 days post-dust exposure. However, meaningful interpretation of these toxicological effects in reduced gravity requires knowledge of the site and the amount of aerosol deposition in the respiratory tract under realistic exposure conditions (aerosolized dust as opposed to tracheal instillation) (37).

A major factor contributing to the pulmonary toxicity of deposited particles is their retention time in the lung air spaces. Particles that deposit in the conducting airways are mainly removed by mucociliary clearance, while most of the particles that deposit in the alveolar region are phagocytized and cleared by alveolar macrophages. The rate of these clearance mechanisms differs by several orders of magnitude, with mucociliary clearance being very much the faster process (half-life of hours/day vs. months/years) (25, 36). Because of the similar levels of $DEP_{peripheral}$ at both gravity levels, our data suggest that toxicological studies of extraterrestrial dust in the fine range (0.5–2 μm) that are performed in a terrestrial laboratory (i.e., in 1G) by aerosol exposure likely provides a good surrogate for investigating potential effects of inhaled particulates to the health of human explorers to the moon or other extraterrestrial bodies. This speculation is based on the reasonable assumption that most of the toxicity of inhaled dust results from the particles that deposited in the lung periphery where clearance rates are low.

In summary, this study reports the effect of gravity on the deposition patterns of fine particles (~1 μm) in the rat lung. Deposition was determined postmortem using MRI after spontaneously breathing rats were exposed to aerosol either in μG or in 1G. Data show that, while in 1G, deposition was relatively uniform between the central and peripheral region of the lung; most particles that deposited in μG did so in the lung periphery. As a consequence, C/P was reduced in μG compared with 1G. Also, although overall deposition tended to be less in μG than in 1G, $DEP_{peripheral}$ was similar in both gravity levels. These data suggest that potential toxicological effects of aerosol exposure in a low gravity environment, such as the surface of the Moon, may not be reduced compared with 1G.

ACKNOWLEDGMENTS

We acknowledge the technical support of Trevor Cooper and Janelle Fine at UCSD, and of Noel Skinner, Wanda Thompson, Dominic Del Rosso, and the reduced gravity office at National Aeronautics and Space Administration-Johnson Space Center (NASA-JSC). We are also gratefully acknowledge the efforts of Stephanie Basset at NASA-JSC for assistance in caring for the animals while housed at JSC, and in assisting with the considerable logistical challenges posed by these studies.

GRANTS

This work was supported by the National Space Biomedical Research Institute through NASA NCC 9–58; by the National Center for Research Resources Grant 5R21RR021919-02; by National Heart, Lung, and Blood Institute Grant 1R21-HL-087805-02 and by National Science Foundation Fellowships (to M. G. Borja and J. M. Oakes).

DISCLOSURES

No conflicts of interest, financial or otherwise, are declared by the author(s).

AUTHOR CONTRIBUTIONS

Author contributions: C.D., E.C.B., I.M.O., and G.K.P. conception and design of research; C.D., J.M.O., E.C.B., I.M.O., M.S., and G.K.P. performed experiments; C.D., M.G.B., J.M.O., and M.S. analyzed data; C.D., E.C.B., I.M.O., M.S., and G.K.P. interpreted results of experiments; C.D. prepared figures; C.D. drafted manuscript; C.D., J.M.O., E.C.B., I.M.O., M.S., and G.K.P. edited and revised manuscript; C.D., M.G.B., J.M.O., E.C.B., I.M.O., M.S., and G.K.P. approved final version of manuscript.

REFERENCES

1. **Brown JS, Wilson WE, Grant LD.** Dosimetric comparison of particle deposition and retention in rats and humans. *Inhal Toxicol* 17: 355–385, 2005.
2. **Butler JP, Tsuda A.** Effect of convective stretching and folding on aerosol mixing deep in the lung, assessed by approximate entropy. *J Appl Physiol* 83: 800–809, 1997.
3. **Cain JR.** Lunar dust: the hazard and astronaut exposure risks. *Earth Moon Planets* 107: 107–125, 2010.
4. **Carpenter JD, Angerer O, Durante M, Linnarsson D, Pike WT.** Life sciences investigations for ESA's first lunar lander. *Earth Moon Planets* 107: 11–23, 2010.
5. **Darquenne C.** Aerosol deposition in the human lung in reduced gravity. *J Aerosol Med Pulm Drug Deliv* 27: 170–177, 2014.
6. **Darquenne C.** Heterogeneity of aerosol deposition in a two-dimensional model of human alveolated ducts. *J Aerosol Sci* 33: 1261–1278, 2002.
7. **Darquenne C, Paiva M, Prisk GK.** Effect of gravity on aerosol dispersion and deposition in the human lung after periods of breath-holding. *J Appl Physiol* 89: 1787–1792, 2000.
8. **Darquenne C, Paiva M, West JB, Prisk GK.** Effect of microgravity and hypergravity on deposition of 0.5- to 3-μm-diameter aerosol in the human lung. *J Appl Physiol* 83: 2029–2036, 1997.
9. **Darquenne C, Prisk GK.** Deposition of inhaled particles in the human lung is more peripheral in lunar than in normal gravity. *Eur J Appl Physiol* 103: 687–695, 2008.
10. **Darquenne C, Prisk GK.** Effect of small flow reversals on aerosol mixing in the alveolar region of the human lung. *J Appl Physiol* 97: 2083–2089, 2004.
11. **Darquenne C, Prisk GK.** Particulate deposition in the human lung under lunar habitat conditions. *Aviat Space Environ Med* 84: 190–195, 2013.
12. **Darquenne C, West JB, Prisk GK.** Deposition and dispersion of 1 μm aerosol boluses in the human lung: effect of micro- and hypergravity. *J Appl Physiol* 85: 1252–1259, 1998.

13. **Darquenne C, West JB, Prisk GK.** Dispersion of 0.5–2 μm aerosol in μG and hypergravity as a probe of convective inhomogeneity in the lung. *J Appl Physiol* 86: 1402–1409, 1999.
14. **Darquenne C, Zeman KL, Sa RC, Cooper TK, Fine JM, Bennett WD, Prisk GK.** Removal of sedimentation decreases relative deposition of coarse particles in the lung periphery. *J Appl Physiol* 115: 546–555, 2013.
15. **Gaier JR.** *The Effect of Lunar Dust on EVA Systems During the Apollo Missions*. Houston, TX: NASA, 2005. (NASA/TM-2005-213610).
16. **Galvin I, Drummond GB, Nirmalan M.** Distribution of blood flow and ventilation in the lung: gravity is not the only factor. *Br J Anaesth* 98: 420–428, 2007.
17. **Graf JC.** *Lunar Soil Size Catalog*. Houston, TX: NASA, 1993 (NASA-RP-1265).
18. **Haber S, Yitzhak D, Tsuda A.** Trajectories and deposition sites of spherical particles moving inside rhythmically expanding alveoli under gravity-free conditions. *J Aerosol Med Pulm Drug Deliv* 23: 405–413, 2010.
19. **Heyder J, Blanchard JD, Feldman HA, Brain JD.** Convective mixing in human respiratory tract: estimates with aerosol boli. *J Appl Physiol* 64: 1273–1278, 1988.
20. **ICRP.** Human respiratory tract model for radiological protection: a report of the task group of the International Commission on Radiological Protection. ICRP Publication 66 Annexe F (reference values for regional deposition). *Ann ICRP* 24: 415–432, 1994.
21. **Lam CW, James JT, Latch JN, Hamilton RF Jr, Holian A.** Pulmonary toxicity of simulated lunar and Martian dusts in mice: II. Biomarkers of acute responses after intratracheal instillation. *Inhal Toxicol* 14: 917–928, 2002.
22. **Lam CW, James JT, McCluskey R, Cowper S, Balis J, Muro-Cacho C.** Pulmonary toxicity of simulated lunar and Martian dusts in mice. I. Histopathology 7 and 90 days after intratracheal instillation. *Inhal Toxicol* 14: 901–916, 2002.
23. **Linnarsson D, Carpenter J, Fubini B, Gerde P, Karlsson LL, Loftus DJ, Prisk GK, Staufer U, Tranfield EM, van Westrenen W.** Toxicity of lunar dust. *Planet Space Sci* 74: 57–71, 2012.
24. **Ma B, Darquenne C.** Aerosol deposition characteristics in distal acinar airways under cyclic breathing conditions. *J Appl Physiol* 110: 1271–1282, 2011.
25. **Moller W, Haussinger K, Winkler-Heil R, Stahlhofen W, Meyer T, Hofmann W, Heyder J.** Mucociliary and long-term particle clearance in the airways of healthy nonsmoker subjects. *J Appl Physiol* 97: 2200–2206, 2004.
26. **Oakes JM, Breen EC, Scadeng M, Tchantchou GS, Darquenne C.** MRI-based measurements of aerosol deposition in the lung of healthy and elastase-treated rats. *J Appl Physiol* 116: 1561–1568, 2014.
27. **Oakes JM, Scadeng M, Breen EC, Marsden AL, Darquenne C.** Rat airway morphometry measured from in situ MRI-based geometric models. *J Appl Physiol* 112: 1921–1931, 2012.
28. **Oakes JM, Scadeng M, Breen EC, Prisk GK, Darquenne C.** Regional distribution of aerosol deposition in rat lungs using magnetic resonance imaging. *Ann Biomed Eng* 41: 967–978, 2013.
29. **Park SS, Wexler AS.** Particle deposition in the pulmonary region of the human lung: multiple breath aerosol transport and deposition. *J Aerosol Sci* 38: 509–519, 2007.
30. **Prisk GK, Sá RC, Darquenne C.** Cardiogenic mixing increases aerosol deposition in the human lung in the absence of gravity. *Acta Astronaut* 92: 15–20, 2013.
31. **Raabe OG, Yeh HC, Newton GJ, Phalen RF, Velasquez DJ.** Deposition of inhaled monodisperse aerosols in small rodents. In: *Inhaled Particles IV*, edited by Walton WH. New York: Pergamon, 1977, p. 3–21.
32. **Rooney D, Friese M, Fraser JF, Dunster KR, Schibler A.** Gravity-dependent ventilation distribution in rats measured with electrical impedance tomography. *Physiol Meas* 30: 1075–1085, 2009.
33. **Rosenthal FS.** The effect on nonuniform ventilation on the dispersion of inspired aerosol boluses–a modeling study. *J Aerosol Med* 6: 177–197, 1993.
34. **Scherer PW, Haselton FR.** Convective exchange in oscillatory flow through bronchial-tree models. *J Appl Physiol* 53: 1023–1033, 1982.
35. **Scheuch G, Stahlhofen W.** Effect of heart rate on aerosol recovery and dispersion in human conducting airways after periods of breathholding. *Exp Lung Res* 17: 763–787, 1991.
36. **Scheuch G, Stahlhofen W, Heyder J.** An approach to deposition and clearance measurements in human airways. *J Aerosol Med* 9: 35–41, 1996.
37. **Scully RR, Lam CW, James JT.** Estimating safe human exposure levels for lunar dust using benchmark dose modeling of data from inhalation studies in rats. *Inhal Toxicol* 25: 785–793, 2013.
38. **Tsuda A, Rogers RA, Hydon PE, Butler JP.** Chaotic mixing deep in the lung. *Proc Natl Acad Sci USA* 99: 10173–10178, 2002.
39. **Weibel ER, Sapoval B, Filoche M.** Design of peripheral airways for efficient gas exchange. *Respir Physiol Neurobiol* 148: 3–21, 2005.